Article

Unveiling the Biocompatible Properties of Date Palm Tree (*Phoenix dactylifera L.*) Biomass-Derived Lignin Nanoparticles

Jegan Athinarayanan, Vaiyapuri Subbarayan Periasamy, and Ali A. Alshatwi*

Read Online

ACCESS | Metrics & More | Article Recommendations

ABSTRACT: Searching for sustainable, ecofriendly, and renewable precursors for nanostructured material synthesis is a fascinating area pertaining to feasibility in various applications. Especially, lignin-based material preparation is essential for unraveling the usage of lignin by valorization. Hence, we have synthesized lignin nanoparticles (LNPs) using date palm tree (*Phoenix dactylifera L.*) biomass as a precursor in this investigation. The LNP's morphological and thermal features were assessed. Moreover, we have evaluated the LNP's cytocompatibility properties by adopting in vitro approach. The *P. dactylifera L.* (PD) biomass-derived LNP's morphological features show a spherical shape with a 10−100 nm diameter. The LNPs have a decreased cell viability of ∼8% at a high concentration exposure to human mesenchymal stem cells (hMSCs) for 48 h. However, the LNPs do not cause any cellular and nuclear morphology changes in hMSCs. The mitochondrial membrane potential assessment results confirm healthy mitochondria with high mitochondrial membrane potential in LNP-treated cells. The intracellular reactive oxygen species (ROS) generation assay results revealed that LNPs do not trigger ROS generation in hMSCs. We examined the upregulation of GSTM3 and GSR genes and the downregulation of SOD1 genes in LNP-treated hMSCs, but no significant changes were observed. Our study concluded that PD biomass-derived LNPs have a good cytocompatibility and an antioxidant property. Thus, they can be applicable for various biological, cosmetic, and environmental applications.
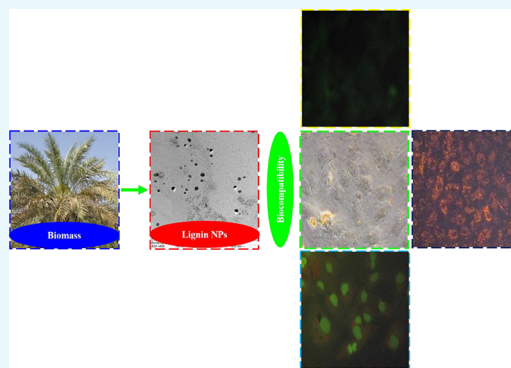
1. INTRODUCTION

The existence of large quantity sustainable, renewable, and ecofriendly biomass and its inept usage is the main challenge worldwide. Agricultural residue generation has been inevitable during agroindustrial activities. Mainly, the agroindustrial residues are lignocellulosic materials.[1,2] Interestingly, lignocellulosic materials are comprised of lignin, cellulose, hemicellulose, and other substances.[3] Lignin is the second most prolific natural biopolymer after cellulose. It is a three-dimensional, highly branched, complex polymer derivative of three different phenylpropane units: sinapyl, coniferyl, and *p*-coumaryl alcohol. Owing to the radical polymerization of these three monolignols creates syringyl (S), guaiacyl (G), and *p*-hydroxyphenyl (H) units. The proportions of the three phenylpropanoid alcohols (S, G, and H) differ for lignin of different origins. Lignin is generated ∼70 million tons per year from different lignocellulosic biomass-utilizing industries.[4] Owing to its high heating value, lignin has been used as a fuel source,[5] but a vast quantity of lignin is not effectively utilized due to unknown knowledge about the full potential of lignin.[6,7] Lignin structural and chemical properties depend on its source and extraction methodologies.[8] Also, these diverse types of lignin exhibit dissimilar deviations in molecular weight, elemental composition, and functional groups. Interestingly,

lignin is a cheap aromatic polymer with unique features, including a high stiffness, thermal stability, high amount of carbon, biodegradability, biocompatibility, and antioxidant and antimicrobial activities.[8−10] These merits raised the concern among scientific communities for transforming lignin into high-value products to be exploited for various purposes.[8] In this aspect, the use of lignin in more cutting-edge applications has increased swiftly. Recently, the use of lignin in lignin nanostructure production is one way for lignin valorization. Fascinatingly, lignin nanoparticles (LNPs) possess multi-potential; thus, they are utilized in drug delivery, nanoglue, functional surface coatings, and microfluidic devices.[11] Generally, the LNPs have been fabricated using a two-step approach: (1) solubilization and (2) precipitation. Lignin is an insoluble substance in water, which is a great challenge in fabricating LNPs for large-scale applications. Previous studies reported that lignin

was dissolved in different organic solvents for the LNP fabrication, such as tetrahydrofuran (THF), ethylene glycol, *N,N*-dimethylformamide (DMF), and acetone.[11−15] The lignin solution was precipitated through different approaches, including the dialysis process, acids, and antisolvents.[11,13,15] Moreover, some of the methods utilized toxic chemicals for LNP preparation, such as pyridine and toluene diisocyanate.[14,16] Thus, alternative approaches for LNP preparation need to be explored to minimize the hazardous chemical usage and maintain the nativity of the functional groups.

The toxicology behavior of nanostructured materials (NMs) is a significant concern in the biomedical sector.[17−20] Currently, a few studies demonstrated that the LNPs have been explored in biomedical applications. For instance, Figueiredo et al. reported that LNP-based iron nanosystems had been utilized for drug delivery for cancer therapy.[21] Chai et al. suggested that chitosan/ lignin hybrid nanoparticles have been exploited for docetaxel and curcumin delivery.[22] A few earlier studies reported that LNPs exhibited biocompatibility in different in vitro models. Nevertheless, any surface chemistry changes are possible to disturb the physicochemical characters of the NMs vital for the cytocompatibility and cellular interfaces, including morphology, surface functional groups, crystalline nature, and particle size distribution. Thus, the cytocompatibility of any new NMs should be carefully assessed in advance food, biomedical and cosmetic industrial usage.[23−31]

In Saudi Arabia, different kinds of plant biomass have been generated, including olive, Washingtonia, Conocarpus, and date palm. Among these, the date palm is a significant tree in Saudi Arabia. Interestingly, the date palm tree (*Phoenix dactylifera L.*) is a vital plant in gulf countries that belongs to the Arecaceae family. Around 100 million date trees are growing worldwide.[3,25,26] A vast amount of biomass from the date palm trees is produced every year, but that biomass is not exploited appropriately. Interestingly, date palm lignocellulosic biomass is inexpensive and readily available as a bioprecursor for LNP preparation. Still, the date palm lignocellulosic biomass-derived LNP's cytotoxic and antioxidant behavior was not well-studied. It is essential to explore the biological properties. Hence, we have synthesized lignin nanoparticles utilizing date palm tree biomass as a precursor in this present study. Furthermore, the LNP biocompatibility was assessed at the molecular level by adopting an in vitro methodology using human mesenchymal stem cells as the in vitro model.

2. MATERIALS AND METHODS

2.1. Materials. Hydrochloric acid, sodium hydroxide, and ascorbic acid were procured from Loba Chemicals, Mumbai, India. 3-(4,5-dimethylthiazol-2-yl)-2,5-diphenyltetrazolium bromide (MTT), 1,1-diphenyl-2-picrylhydrazyl (DPPH), strep-tomycin/penicillin antibiotics, fetal bovine serum, 5,5,6,6′-tetrachloro-1,1′,3,3′ tetraethylbenzimidazoylcarbocyanine io-dide (JC-1) dye, acridine orange (AO) and ethidium bromide (EB) were purchased from Sigma-Aldrich Inc., USA. Dulbecco's modified Eagle medium (DMEM) was purchased from Invitrogen, USA.

2.2. Extraction of Lignin from Date Palm Tree Biomass. The date palm fruit stalk was collected from the local date farm in Riyadh, Saudi Arabia. The obtained biomass was powdered, and lignin was extracted using a previously described method with slight modifications.[32] Around 10 g of the date palm biomass powder was mixed with 200 mL of water and transferred to a Teflon-coated stainless steel autoclave. The

autoclave was kept at 200 °C for 30 min under pressurized conditions. Afterward, the obtained solid residues were mixed with 4% sodium hydroxide and maintained at 140 °C for 3 h. Then, the black liquid was separated by filtration. After that, lignin was precipitated using 0.1 M HCl to acidify the black liquid to pH 2.0. The obtained precipitation was washed with water until the removal of acid residues. The purified lignin was dried at ambient temperature.

2.3. Fabrication of Lignin Nanoparticles. The date palm biomass-derived lignin was used to synthesize lignin nano-particles. About 250 mg of lignin was dissolved in 50 mL of THF and centrifuged at 8000 rpm for 2 min. Subsequently, the lignin solution was loaded into a dialysis bag. Afterward, the bag was placed in distilled water for 24 h under stirring. Every 4 h interval, the distilled water was changed. After dialysis, the obtained sample was dried and used for further studies.

2.4. Characterization of Lignin Samples. The optical property of lignin and its nanostructures were examined by adopting UV−visible near-infrared spectroscopy (Agilent, Saudi Arabia). The chemical properties of the samples were investigated using FT-IR spectroscopy (PerkinElmer Model) at 4000−500 cm^{-1}. The average particle size distribution of the LNPs was examined using Zetasizer (Nano-ZS90, Malvern, UK). The morphological characteristics of the LNPs were studied using a transmission electron microscope. The date palm biomass-derived LNP thermal stability behavior was evaluated by adopting a thermogravimetric analyzer (Model, USA).

2.5. Assessment of Cytocompatibility of the Lignin Nanoparticles. *2.5.1. Culture of Cells.* hMSCs were acquired from ATCC, USA. DMEM with 1% antibiotics (penicillin/ streptomycin [100U/100 μg/mL]) and 10% fetal bovine serum was used for hMSCs cultivation at 37 °C and a 5% CO$_2$ environment.

2.5.2. Cell Viability Assay. The cytotoxic effect of LNPs on hMSCs was determined using an MTT assay. After hMSCs adhesion, the cell culture media was discarded and replenished with different doses of LNPs (control, 12.5, 25, 50, 100, and 200 μg/mL) in cell culture media. The plate was incubated for 24 and 48 h. After incubation, 20 μL of the MTT solution (5.0 mg/ mL of PBS) was added per well. Then, the plate was incubated in the dark at 37 °C for 6 h. Afterward, the media was discarded carefully, and formazan crystals were dissolved in 200 μL of dimethyl sulfoxide. The plate absorbance was read using a microplate reader at 570 and 630 nm (reference wavelength). The cell viability was calculated from obtained data using the following formula

$$\text{cell viability} = \frac{\text{mean OD of treated cells}}{\text{mean OD of untreated cells (control)}} \times 100$$

2.5.3. Analysis of Cell and Nuclear Morphological Changes. After cell adhesion in a 12-well plate, the hMSCs were treated with different doses of LNPs (50 and 100 μg/mL) for 24 and 48 h. Then, the hMSC cellular morphology was observed under a bright-field microscope. The cells were stained with an AO/EB (100 μg each) dye for observation of the nuclear morphology and watched under epifluorescence microscopy.

2.5.4. Mitochondrial Membrane Potential Assessment. hMSCs were exposed to different doses of LNPs (50 and 100 μg/mL) in 12-well plates for 24 and 48 h. The assay was carried out as per the manufacturer's instructions (BD Biosciences, USA). After a 24 h treatment, the hMSCs were washed with the assay buffer. Subsequently, the JC-1 was added to each well and

Scheme 1. Schematic Flow Diagram for Lignin Nanoparticle Fabrication from Date Palm Fruit Stalk Biomass
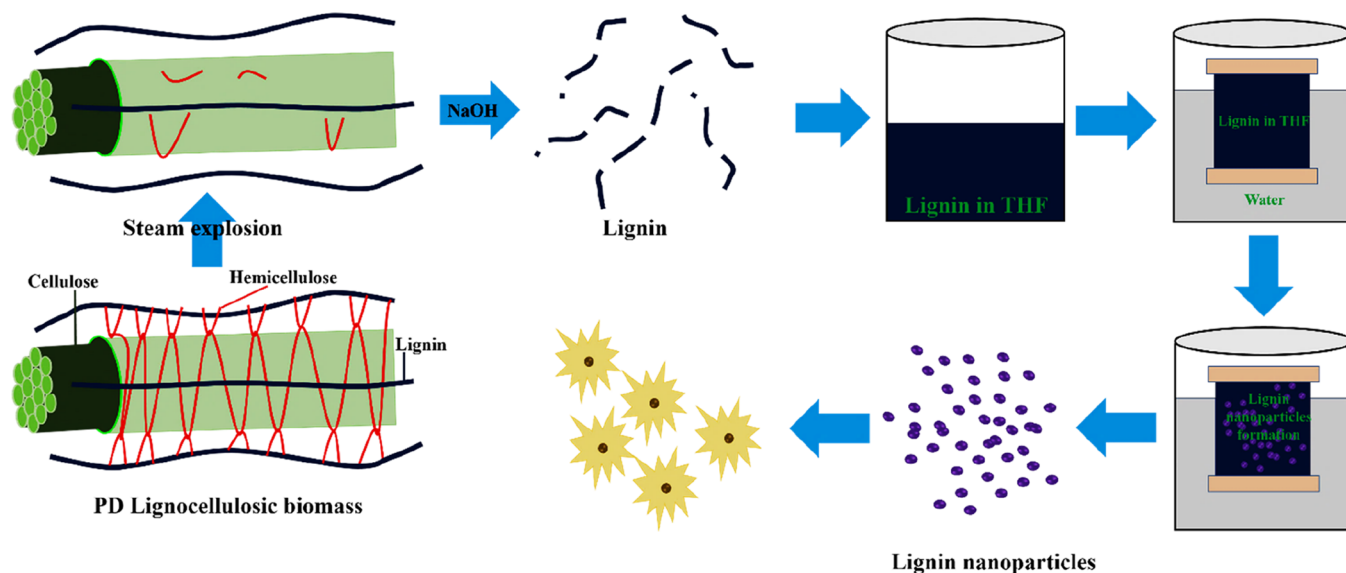
kept in the dark for 20 min at 37 °C. After staining, cells were washed with the assay buffer and imaged under a fluorescence microscope with a high-efficiency filter at 515/545 and 575/625 nm.

2.5.5. Intracellular ROS Generation. According to manufacturer instructions, an intracellular ROS measurement for lignin and LNPs exposed on hMSCs was determined using an H_2DCFDA fluorescent probe. The fluorescent probe easily penetrates the cell membrane and transforms into a non-fluorescent substance. As per the intracellular ROS level, 2,7-dichlorofluorescein is converted into the highly fluorescent 2,7-dichlorofluorescein (DCF). After lignin and LNPs exposure, the cells were washed and added to the DCFDA dye. Then, the cells were incubated at 37 °C for 45 min in the dark. After incubation, the cells were examined under a fluorescence microscope and captured images.

2.5.6. Gene Expression Analysis. The influence of LNPs on the hMSC gene expression was studied using a reverse transcription-polymerase chain reaction using the real-time SYBR Green gene expression assay kit (QIAGEN, Germany). The lignin- and LNP-exposed cells' cDNA was synthesized using the Fastlane Cell cDNA kit. The mRNA levels of GSR, CAT, SOD1, GSTM3, GSTA4, and FAS genes were determined using glyceraldehyde 3-phosphate dehydrogenase (GAPDH) as the reference gene. A total of 25 μL of the PCR reaction mix composed of 500 ng of template cDNA (2 μL), master mix (12.5 μL), RNase-free water (8.5 μL), and primers (2 μL) was added per well. After that, the plate was subjected to an RT-PCR machine for 40 cycles.[33] Subsequently, the results were calculated by a comparative threshold (C_t) method, and fold changes were compared with the control. The mRNA level of expression of the target genes was analyzed by the Athinarayanan et al. method.[34] The ratio of the reference gene expression to target gene expression levels was measured as $\Delta C_t = C_t$ (target genes) $- C_t$ (GAPDH) and $\Delta\Delta C_t = \Delta C_t$ (treated) $- \Delta C_t$ (control), respectively. The obtained data were used to plot the target gene expression using the values of $2^{-\Delta\Delta C_t}$.

2.6. Statistical Analysis. The values are shown as mean ± standard deviation. The values were calculated using Microsoft Excel software (Microsoft Corp., KY, USA). A value of $p < 0.05$ was considered statistically significant.

3. RESULTS AND DISCUSSION

3.1. Characterization of Lignin Nanoparticles. Lignin is a structurally three-dimensional, highly branched aromatic, and heterogeneous biomacromolecule occurring in the plant's cell walls.[32] Lignin is the second most existing biopolymer whose structural and chemical features depend on source and extraction methodologies.[8] The *P. dactylifera*-derived lignin nanoparticles (LNPs) have free radical scavenging potential and cytotoxic features, which are still unknown. Thus, we have extracted lignin from *P. dactylifera* fruit stalk biomass in this present investigation and fabricated lignin nanostructures. Furthermore, we have assessed the *P. dactylifera*-derived LNP's cytotoxic and free radical scavenging potential using an in vitro approach.

Scheme 1 represents the LNP fabrication flow diagram from *P. dactylifera* fruit stalk biomass through a sequential process including steam explosion, alkali treatment, and dialysis steps. The date fruit stalk is mainly composed of hemicellulose, cellulose, and lignin. The lignin and hemicellulose network embed the cellulosic fibrils. At the steam explosion, the date fruit stalk containing hemicellulose was released. The remaining biomass was exposed to alkali treatment under pressurized conditions, whereas lignin molecules were solubilized in alkaline media. After that, the lignin fraction was precipitated by acidification. The obtained date fruit stalk lignin was used as a precursor for LNP fabrication. The THF dissolved the lignin molecules and dialyzed against water. The THF was swapped with water during the dialysis process, and lignin NPs were formed through a nucleation growth mechanism. Lievonen et al. proposed a similar mechanism for LNP formation in a dialysis bag.[11] Also, previous studies demonstrated that the lignin concentration in the dialysis process had played an essential role in the lignin particle size. At a high lignin concentration, the dialysis process leads to a fast nucleation growth and formation of different sizes of LNPs.[11]

The optical behavior of LNPs was studied using UV−vis spectroscopy. Figure 1 depicts the UV spectra of date fruit stalk-derived LNPs. The UV spectra of the date fruit stalk-derived lignin and LNPs displayed absorption maxima at 284 nm ascribed to nonconjugated phenolic groups or aromatic rings of
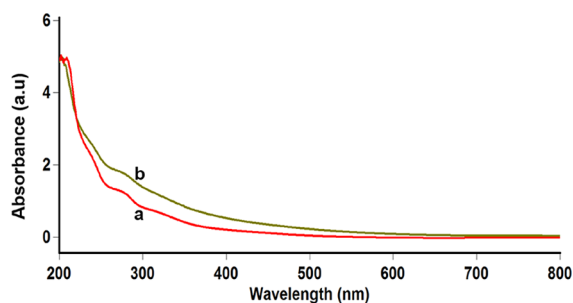
Figure 1. UV−visible spectra of date palm fruit stalk-derived (a) lignin and (b) lignin nanoparticles.

guaiacyl units in lignin.[35,36] Also, the results suggested that date fruit stalk-derived lignin has a high guaiacyl content.[36] Earlier studies' results agree well with the present study.[36]

The FTIR spectra of the lignin and LNPs are shown in Figure 2. We observed several absorption bands in lignin and LNPs.
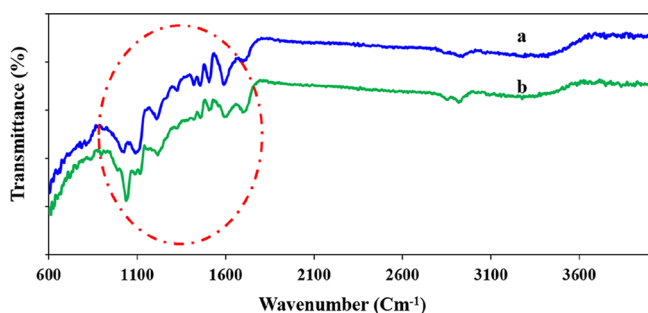

Figure 2. FTIR spectra of date palm fruit stalk-derived (a) lignin and (b) lignin nanoparticles at 4000−600 cm^{-1}.

The broad band was observed between 3500−3300 cm^{-1}, which is ascribed to the stretching of the O−H group. The peak between 2950 and 2800 cm−1 corresponds to the C−H stretching of aromatic methoxyl and methyl groups (symmetric and asymmetric) in lignin and LNPs.[35] Moreover, the band around 1713 cm-1 is associated with the C=O stretching of aldehydes. In Figure 3, the FTIR spectra focus on the regions between 800−1800 cm−1. It shows the peak between 1500−1400 cm-1 is attributed to aromatic ring vibration. 1456 and 1419 cm-1 are specifically responsible for C−H deformations and aromatic skeletal vibrations, respectively. Additionally, the band around 1325 cm-1 is observed in lignin and LNPs, corresponding to syringyl (S) and guaiacyl (G) aromatic ring
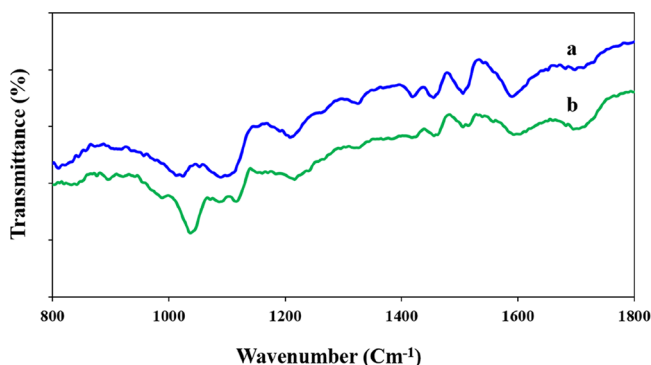

Figure 3. FTIR spectra of date palm fruit stalk-derived (a) lignin and (b) lignin nanoparticles at 1800−800 cm^{-1}.

breathing. The bands at 1262 and 1213 cm-1 are assigned to guaiacyl unit breathing with C=O stretching and aromatic ring breathing with C−C, C−O, and C=O stretching, respectively. Additionally, the absorption peaks around 1117 and 1036 cm^{-1} correspond to aromatic ring C−H in-plane deformation of syringyl (S) and guaiacyl (G) units.[32]

To acquire knowledge about LNP's thermal stability, we have assessed thermogravimetric analysis (Figure 4). We observed
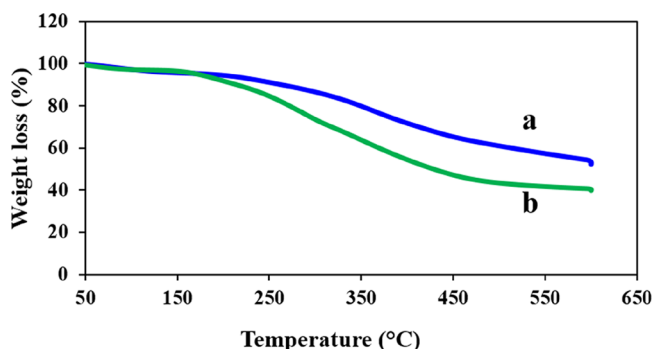

Figure 4. Thermogravimetric analysis of date palm fruit stalk-derived (a) lignin and (b) lignin nanoparticles.

that date fruit stalk lignin and LNPs weight was unchanged initially. At 100 °C, 3% of weight loss was observed in both lignin and LNPs, removing water molecules from their surfaces. After this stage, the weight loss was occurring in lignin and LNPs in three steps such as 150−200 °C (removal of hydroxyl groups), 200−400 °C for the disintegration of interbond linkages, and 400−600 °C for the decomposition of aromatic rings and C−C linkages in lignin.[37] At 200 °C, around 6 and 9% of weight loss were observed in lignin and LNPs, respectively. Interestingly, at 400 °C, 29 and 46% of weight loss were observed due to degradation of aryl ether bond linkages.[38] At 600 °C, 61 and 48% of weight loss were found in lignin and LNPs, respectively, whereas the C−C linkages and aromatic rings were degraded above 400 °C. Our thermal behavior study results suggested that lignin has a high thermostability than LNPs.

The prepared LNP's crystalline nature was assessed using an X-ray diffractometer. The XRD pattern of LNPs is shown in Figure 5. It displays a broad peak around the 2θ value of 22.04°. This result confirmed that LNPs have an amorphous nature. Earlier study results were well-matched with the present study.[39]

The structural and morphological features of the prepared LNPs were investigated using a transmission electron microscope (Figure 6). The TEM images exhibit well-dispersed LNPs
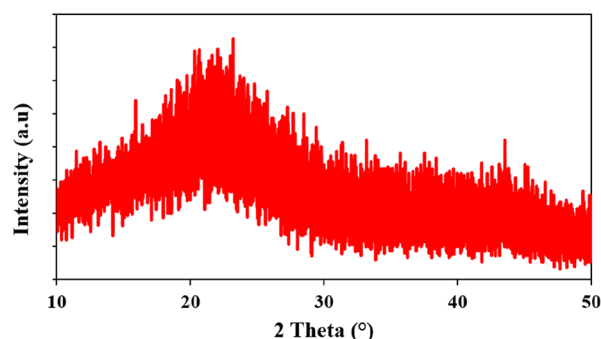

Figure 5. X-ray diffraction pattern of date palm fruit stalk-derived lignin nanoparticles.
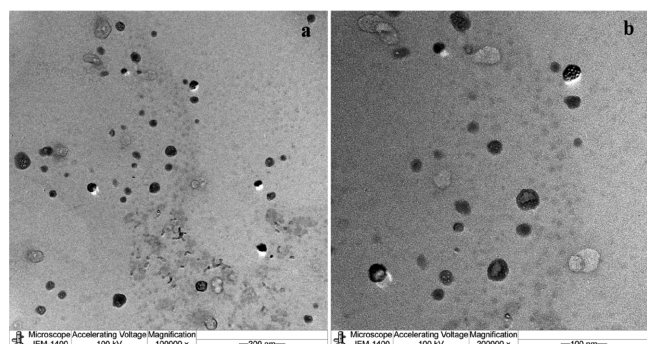
Figure 6. Transmission electron microscopy image of date palm fruit stalk-derived lignin nanoparticles at different magnifications.

with 10−100 nm in diameter spherical particles. Luo et al. study demonstrated that the LNP yield, stability, structure, and morphology depend on the lignin concentration.[40] Dynamic light scattering (DLS) is an important technique used to measure the average particle size of nanoparticles in liquids. The prepared LNP particle size distribution and zeta potential were studied (Figure 7). The DLS results indicate that date palm fruit stalk-derived LNP's average particle size is 142.9 nm (Figure 7a). The obtained average particle size of LNPs is higher than that obtained from the TEM analyses due to aggregation.[41] The stability of LNPs is an essential behavior for a superior usage in different applications.[42] Interestingly, the zeta potential of the prepared LNP dispersion is −27.1, and the results suggest that LNPs are highly stable in water (Figure 7b). Similarly, earlier studies reported that industrial lignin-derived LNPs have a high zeta potential and an excellent water stability.[40,42] The outstanding stability of LNPs reveals that they can be applied in various applications.

3.2. Assessment of Lignin Nanoparticles Cytocompatibility. Understanding the cytotoxic and antioxidant behavior of the *P. dactylifera*-derived lignin and LNPs is very important for their usage in the biomedicine and cosmetic industry. Thus, we have assessed the cytotoxic potential of LNPs in hMSCs. After exposure of lignin and LNPs to hMSCs, the cell viability was evaluated. The cell viability was decreased to 92 and 95% at a high concentration of lignin- and LNP-exposed cells after 24 h, respectively (Figure 8). After 48 h exposure, we observed no significant changes compared with 24 h exposure, even though we expected to see over 12% decline in viability, indicating that lignin and LNPs are nontoxic and cytocompatible materials possibly appropriate for biological uses.

We examined the influence of lignin and LNPs on the cell and nuclear morphology, mitochondrial membrane potential, and intracellular ROS level in hMSCs after exposure to various concentrations. The cellular and nuclear morphological assess-

ment results are displayed in Figure 9a,b. The cellular morphology images show healthy, elongated, and confluent cells in control and treated groups (lignin and LNPs). Even with high-dose-exposed cells, no significant changes were observed in the cellular morphology. The images suggested that LNPs have a cellular uptake into the cytoplasm. LNPs easily penetrate through the cellular membrane and accumulate in the cytoplasm when compared with lignin due to a negative zeta potential.

The AO/EB staining results suggested that lignin- and LNP-exposed cells have intact nuclei that seem green in color. At the same time, no difference was observed between the lignin- and LNP-exposed and unexposed control groups. Our study results confirm that lignin and LNPs are nontoxic substances that could be suitable for biomedical and cosmetic applications.

Mitochondria is a vital subcellular organelle that acts as a cell powerhouse. It has been involved in cell death and cell life mechanisms by regulating cell signaling, redox status, cell growth, and ion homeostasis.[43] The mitochondrial membrane potential (MMP) is a vital redox marker for healthy cells. The consequences of lignin and LNP exposure on MMP of hMSCs were investigated by JC-1 staining. The normal and MMP-reduced cells appear orange−red and green in color, respectively. We observed that lignin- and LNP-exposed and control cells were orange−red in color, suggesting the nonexistence of the mitochondrial membrane potential loss (Figure 10a), even for high-dose-exposed cells.

ROS are generated as a usual cellular metabolic coproduct in living cells.[44] However, the cells generate a large amount of ROS under stress, and the cells ultimately progress through a sequence of feedback mechanisms. Also, excess ROS molecules would activate oxidative stress in a response mechanism associated with various biological processes, including necrosis, apoptosis, and autophagy.[45] Thus, we have evaluated the intracellular ROS level in hMSCs after lignin and LNP exposure (Figure 10b). We found that lignin and LNP exposure do not modify the intracellular ROS basal levels compared with the control. Earlier studies demonstrated that lignin-based materials have an excellent ROS scavenging property due to their antioxidant potential.[46] Also, lignin contains several hydroxyl groups, increasing its scavenging potential. The study by Liang et al. revealed that lignin/poly (ε-caprolactone) implants decreased ROS generation by triggering the antioxidant enzymes.[47] These study results agree with the earlier studies.[46,47] Overall, microscopic study results were constant with the cell viability study results. Together, these results indicate that lignin and LNPs do not promote any adverse effects in hMSCs. Thus, the date palm-derived lignin and LNPs are nontoxic and cytocompatible materials.

We have assessed the lignin and LNP cytotoxic behavior at the molecular level using gene expression analysis. We have analyzed
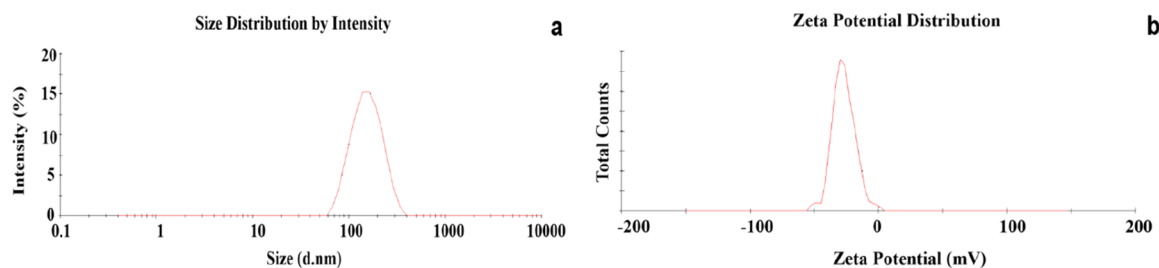

Figure 7. (a) Particle size distribution and (b) zeta potential distribution of date palm fruit stalk-derived lignin nanoparticles.
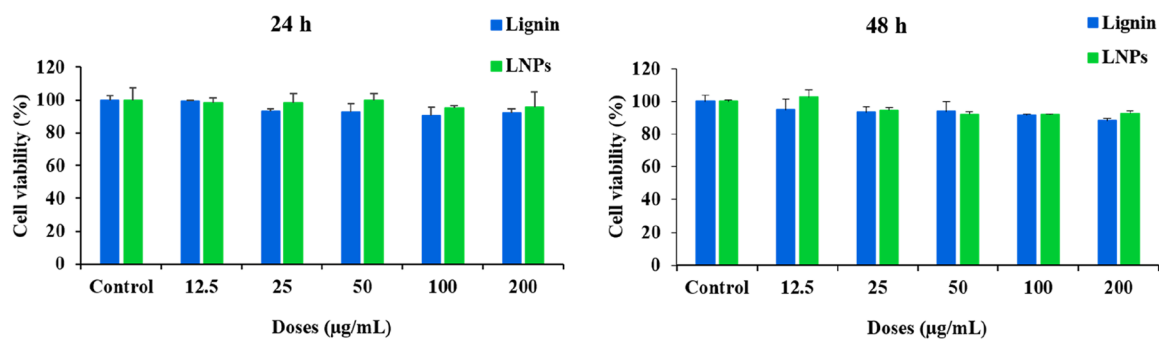
Figure 8. Date palm fruit stalk-derived lignin and lignin nanoparticle's influence on the cell viability of hMSCs.
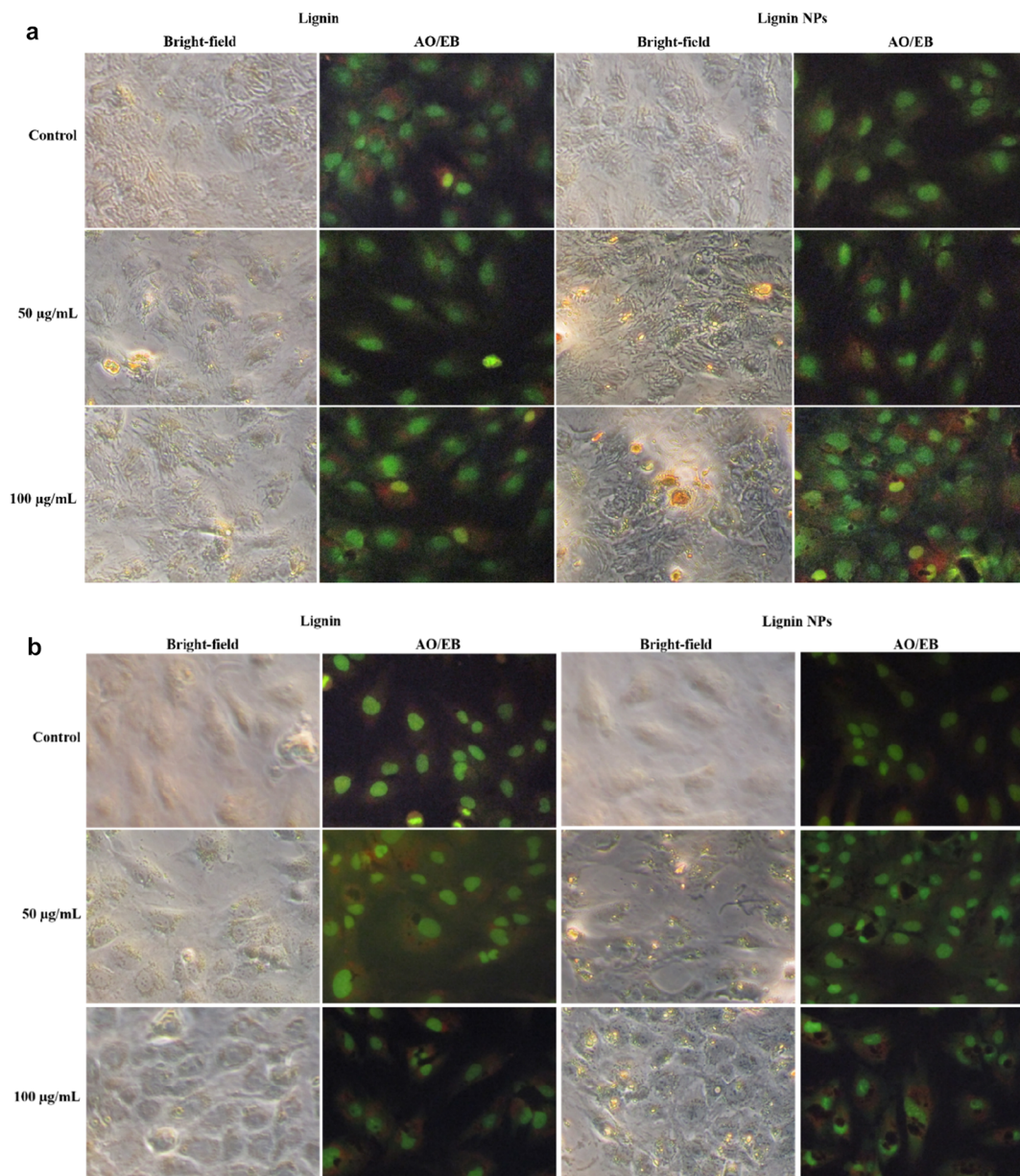

Figure 9. (a) Date palm fruit stalk-derived lignin and lignin nanoparticle's effect on the cellular and nuclear morphology of hMSCs after 24 h. (b) Date palm fruit stalk-derived lignin and lignin nanoparticle's effect on the cellular and nuclear morphology of hMSCs after 48 h.

CAT, SOD1, GSR, GSTM3, GSTA4, and FAS gene expression levels in hMSCs after lignin and LNP exposure (Figure 11). The CAT (catalase), GSR (glutathione S-reductase), SOD1 (superoxide dismutase), GSTM3 (glutathione S-transferase mu 3), and GSTA4 (Glutathione S-transferase A4) genes are antioxidant enzyme genes. The LNPs increase the GSTM3 gene expression level in hMSCs at a low dose compared with control and lignin-exposed cells. We observed a dose-dependent
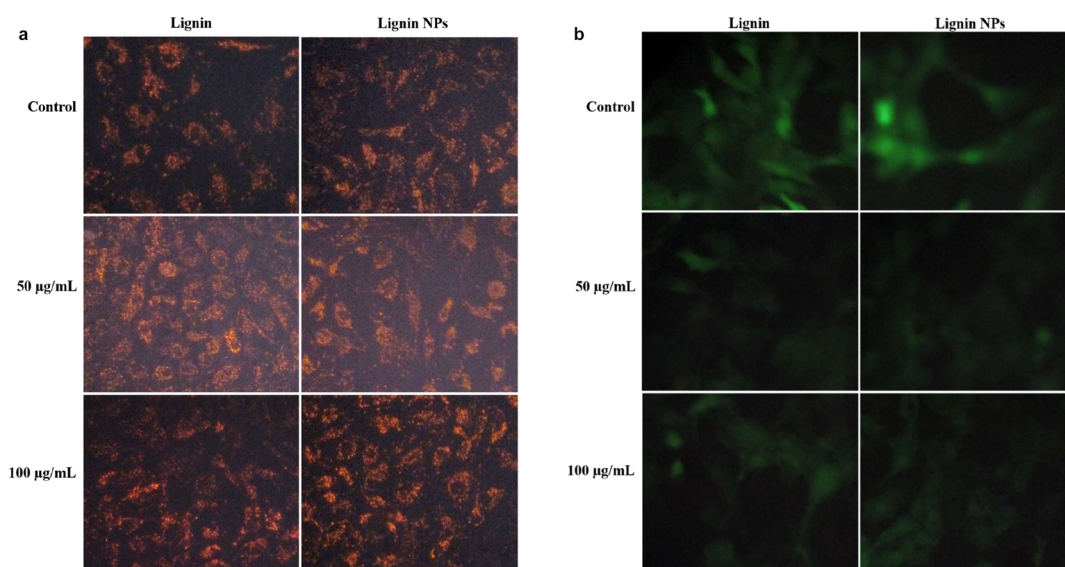
Figure 10. (a) Mitochondrial membrane potential of hMSCs after exposure to date palm fruit stalk-derived lignin and lignin nanoparticles for 24 h. (b) ROS of hMSCs after exposure to date palm fruit stalk-derived lignin and lignin nanoparticles for 24 h.
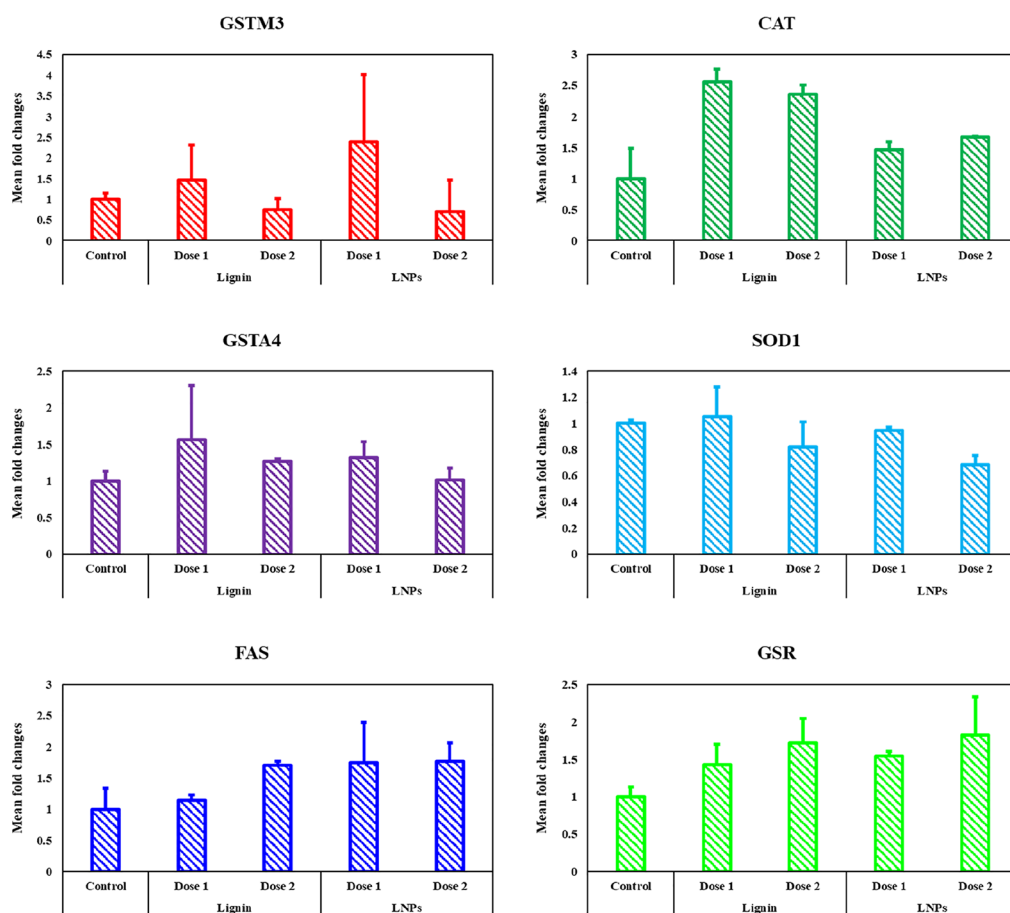

Figure 11. Gene expression level changes as fold change (i.e., the ratio of the target gene to the reference gene, GAPDH) in hMSCs after lignin and lignin nanoparticle exposure for 24 h (dose 1 = 25 μg/mL; dose 2 = 50 μg/mL). Data are the mean ± SD of three determinations, each performed in triplicate.

GSR gene expression in lignin- and LNP-exposed cells. The CAT gene expression level is high in lignin-treated cells. We found dose-dependent downregulation in the SOD gene's expression in lignin- and LNP-treated cells. However, no significant changes were found between the lignin- and LNP-treated cell's gene expression levels, revealing the nontoxicity of LNPs in hMSCs.

The intracellular redox system is a crucial player in cellular homeostasis. A disturbed intracellular signaling and regulation lead to cell death, abnormal mitochondrial physiology, damaged

intracellular DNA and cell cycle arrest, and an irregular molecular signaling. Understanding the induced redox mechanism by external agents is directly linked with the cell death mechanisms. For instance, SOD1, CAT, GSTM4, GSTA3, and FAS are crucial markers directly involved in the redox homeostasis and cell death mechanism (Figure 12). We
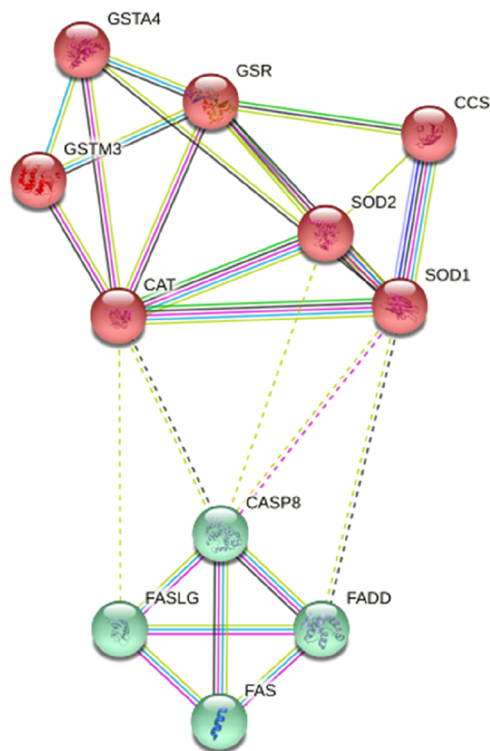

Figure 12. Schematic representation of the gene network of antioxidant and cell death receptor-related genes.

observed downregulation of the SOD1 gene expression in LNP-treated cells. Also, upregulation of the GSR and FAS gene expression was found in lignin- and LNP-exposed cells. Lignin increased the CAT gene expression level when compared to LNPs. Our gene expression study shows no significant changes in the redox markers and surface cell death markers, such as SOD1, CAT, GSTM4, GSTA3, and FAS. It is indicated that LNPs do not disturb the intracellular ROS and mitochondrial physiology in the hMSCs. Overall, our cytocompatibility study results showed that LNPs possess an excellent biocompatibility. It can be suitable for biomedical and cosmetic applications.

4. CONCLUSIONS

The LNPs were synthesized from date palm tree (*P. dactylifera L.*) biomass. The synthesized LNP's morphological, thermal, and cytocompatible features were analyzed using a transmission electron microscope, a thermogravimetric analysis, and an in vitro approach, respectively. The synthesized LNPs are 10−100 nm in size with a spherical shape. The LNPs do not reduce the cell viability above 8%, even at a high concentration exposure. Also, the LNPs exhibited an excellent compatibility in cellular and nuclear morphology analysis in human mesenchymal stem cells (hMSCs). The MMP assay results revealed that LNPs does not alter the MMP. The intracellular ROS generation assay and gene expression results clearly indicate that LNPs have a good cytocompatibility and antioxidant activity. Therefore, LNPs can be appropriate for various biological and cosmetic applications.

AUTHOR INFORMATION

Corresponding Author

Ali A. Alshatwi − *Nanobiotechnology and Molecular Biology Research Laboratory, Department of Food Science and Nutrition, College of Food Science and Agriculture, King Saud University, Riyadh 11451, Saudi Arabia*; Phone: +966 1 467 7122; Email: nano.alshatwi@gmail.com, alshatwi@ksu.edu.sa; Fax: +966 1 467 8394

Authors

Jegan Athinarayanan − *Nanobiotechnology and Molecular Biology Research Laboratory, Department of Food Science and Nutrition, College of Food Science and Agriculture, King Saud University, Riyadh 11451, Saudi Arabia*; orcid.org/0000-0002-0947-2675

Vaiyapuri Subbarayan Periasamy − *Nanobiotechnology and Molecular Biology Research Laboratory, Department of Food Science and Nutrition, College of Food Science and Agriculture, King Saud University, Riyadh 11451, Saudi Arabia*

Complete contact information is available at:
https://pubs.acs.org/10.1021/acsomega.2c00753

Author Contributions

J.A.—conceptualization, methodology, data curation, writing— original draft, visualization, investigation, TOC graphic, and scheme drawing. V.S.P.—methodology, data curation, and review and editing. A.A.A.—conceptualization, review and editing, and supervision.

Notes

The authors declare no competing financial interest.

REFERENCES

(1) De, D.; Naga Sai, M. S.; Aniya, V.; Satyavathi, B. Strategic biorefinery platform for green valorization of agro-industrial residues: A sustainable approach towards biodegradable plastics. *J. Clean. Prod.* **2021**, *290*, 125184.

(2) Sadh, P. K.; Duhan, S.; Duhan, J. S. Agro-industrial wastes and their utilization using solid state fermentation: a review. *Bioresour. Bioprocess.* **2018**, *5*, 1−15.

(3) Athinarayanan, J.; Periasamy, V. S.; Alshatwi, A. A. Phoenix dactylifera lignocellulosic biomass as precursor for nanostructure fabrication using integrated process. *Int. J. Biol. Macromol.* **2019**, *134*, 1179−1186.

(4) Wang, H.; Pu, Y.; Ragauskas, A.; Yang, B. From lignin to valuable products—strategies, challenges, and prospects. *Bioresour. Technol.* **2019**, *271*, 449−461.

(5) Agarwal, A.; Rana, M.; Park, J.-H. Advancement in technologies for the depolymerization of lignin. *Fuel Process. Technol.* **2018**, *181*, 115−132.

(6) Bruijnincx, P. C. A.; Rinaldi, R.; Weckhuysen, B. M. Unlocking the potential of a sleeping giant: lignins as sustainable raw materials for renewable fuels, chemicals and materials. *Green Chem.* **2015**, *17*, 4860−4861.

(7) Low, L. E.; Teh, K. C.; Siva, S. P.; Chew, I. M. L.; Mwangi, W. W.; Chew, C. L.; Goh, B.-H.; Chan, E. S.; Tey, B. T. Lignin nanoparticles: The next green nanoreinforcer with wide opportunity. *Environ. Nanotechnol. Monit. Manag.* **2021**, *15*, 100398.

(8) Kai, D.; Tan, M. J.; Chee, P. L.; Chua, Y. K.; Yap, Y. L.; Loh, X. J. Towards lignin-based functional materials in a sustainable world. *Green Chem.* **2016**, *18*, 1175−1200.

(9) Figueiredo, P.; Lintinen, K.; Hirvonen, J. T.; Kostiainen, M. A.; Santos, H. A. Properties and chemical modifications of lignin: Towards lignin-based nanomaterials for biomedical applications. *Prog. Mater. Sci.* **2018**, *93*, 233−269.

(10) Hu, J.; Zhang, Q.; Lee, D.-J. Kraft lignin biorefinery: A perspective. *Bioresour. Technol.* **2018**, *247*, 1181−1183.

(11) Lievonen, M.; Valle-Delgado, J. J.; Mattinen, M.-L.; Hult, E.-L.; Lintinen, K.; Kostiainen, M. A.; Paananen, A.; Szilvay, G. R.; Setälä, H.; Österberg, M. A simple process for lignin nanoparticle preparation. *Green Chem.* **2016**, *18*, 1416−1422.

(12) Frangville, C.; Rutkevičius, M.; Richter, A. P.; Velev, O. D.; Stoyanov, S. D.; Paunov, V. N. Fabrication of environmentally biodegradable lignin nanoparticles. *ChemPhysChem* **2012**, *13*, 4235.

(13) Richter, A. P.; Bharti, B.; Armstrong, H. B.; Brown, J. S.; Plemmons, D.; Paunov, V. N.; Stoyanov, S. D.; Velev, O. D. Synthesis and characterization of biodegradable lignin nanoparticles with tunable surface properties. *Langmuir* **2016**, *32*, 6468−6477.

(14) Qian, Y.; Zhang, Q.; Qiu, X.; Zhu, S. CO_2-responsive diethylaminoethyl-modified lignin nanoparticles and their application as surfactants for CO_2/N_2-switchable Pickering emulsions. *Green Chem.* **2014**, *16*, 4963−4968.

(15) Myint, A. A.; Lee, H. W.; Seo, B.; Son, W.-S.; Yoon, J.; Yoon, T. J.; Park, H. J.; Yu, J.; Yoon, J.; Lee, Y.-W. One pot synthesis of environmentally friendly lignin nanoparticles with compressed liquid carbon dioxide as an antisolvent. *Green Chem.* **2016**, *18*, 2129−2146.

(16) Yiamsawas, D.; Baier, G.; Thines, E.; Landfester, K.; Wurm, F. R. Biodegradable lignin nanocontainers. *RSC Adv.* **2014**, *4*, 11661−11663.

(17) Athinarayanan, J.; Periasamy, V. S.; Alhazmi, M.; Alatiah, K. A.; Alshatwi, A. A. Synthesis of biogenic silica nanostructures from rice husks for biomedical applications. *Ceram. Int.* **2015**, *41*, 275−281.

(18) Athinarayanan, J.; Periasamy, V. S.; Alshatwi, A. A. Simultaneous fabrication of carbon nanodots and hydroxyapatite nanoparticles from fish scale for biomedical applications. *Mater. Sci. Eng. C* **2020**, *117*, 111313.

(19) Athinarayanan, J.; Alshatwi, A. A.; Subbarayan Periasamy, V. Biocompatibility analysis of Borassus flabellifer biomass-derived nanofibrillated cellulose. *Carbohydr. Polym.* **2020**, *235*, 115961.

(20) Alshatwi, A. A.; Athinarayanan, J.; Periasamy, V. S. Biocompatibility assessment of rice husk-derived biogenic silica nanoparticles for biomedical applications. *Mater. Sci. Eng. C* **2015**, *47*, 8−16.

(21) Figueiredo, P.; Lintinen, K.; Kiriazis, A.; Hynninen, V.; Liu, Z.; Bauleth-Ramos, T.; Rahikkala, A.; Correia, A.; Kohout, T.; Sarmento, B.; Yli-Kauhaluoma, J.; Hirvonen, J.; Ikkala, O.; Kostiainen, M. A.; Santos, H. A. In vitro evaluation of biodegradable lignin-based nanoparticles for drug delivery and enhanced antiproliferation effect in cancer cells. *Biomaterials* **2017**, *121*, 97−108.

(22) Chai, Y.; Wang, Y.; Li, B.; Qi, W.; Su, R.; He, Z. Microfluidic Synthesis of Lignin/Chitosan Nanoparticles for the pH-Responsive Delivery of Anticancer Drugs. *Langmuir* **2021**, *37*, 7219−7226.

(23) Athinarayanan, J.; Periasamy, V. S.; Alhazmi, M.; Alshatwi, A. A. Synthesis and biocompatibility assessment of sugarcane bagasse-derived biogenic silica nanoparticles for biomedical applications. *J. Biomed. Mater. Res., Part B* **2017**, *105*, 340−349.

(24) Athinarayanan, J.; Periasamy, V. S.; Alatiah, K. A.; Alshatwi, A. A. Synthesis and cytocompatibility analysis of carbon nanodots derived from palmyra palm leaf for multicolor imaging applications. *Sustainable Chem. Pharm.* **2020c**, *18*, 100334.

(25) Athinarayanan, J.; Periasamy, V. S.; Alshatwi, A. A. Fabrication of cellulose nanocrystal-decorated hydroxyapatite nanostructures using ultrasonication for biomedical applications. *Biomass Convers. Biorefin.* **2021**, DOI: 10.1007/s13399-021-01481-2.

(26) Athinarayanan, J.; Periasamy, V. S.; Al-Harbi, L. N.; Alshatwi, A. A. Phoenix dactylifera leaf-derived biocompatible carbon quantum dots: application in cell imaging. *Biomass Convers. Biorefin.* **2022**, DOI: 10.1007/s13399-021-02159-5.

(27) Hamad Jaafari, S. A. A.; Athinarayanan, J.; Subbarayan Periasamy, V.; Alshatwi, A. A. Biogenic silica nanostructures derived from Sorghum bicolor induced osteogenic differentiation through BSP, BMP-2 and BMP-4 gene expression. *Process Biochem.* **2020**, *91*, 231−240.

(28) Athinarayanan, J.; Jaafari, S. A. A. H.; Periasamy, V. S.; Almanaa, T. N. A.; Alshatwi, A. A. Fabrication of biogenic silica nanostructures from Sorghum bicolor leaves for food industry applications. *Silicon* **2020d**, *12*, 2829−2836.

(29) Imlimthan, S.; Correia, A.; Figueiredo, P.; Lintinen, K.; Balasubramanian, V.; Airaksinen, A. J.; Kostiainen, M. A.; Santos, H. A.; Sarparanta, M. Systematic in vitro biocompatibility studies of multimodal cellulose nanocrystal and lignin nanoparticles. *J. Biomed. Mater. Res., Part A* **2020**, *108*, 770−783.

(30) Periasamy, V. S.; Athinarayanan, J.; Alshatwi, A. A. Anticancer activity of an ultrasonic nanoemulsion formulation of Nigella sativa L. essential oil on human breast cancer cells. *Ultrason. Sonochem.* **2016**, *31*, 449−455.

(31) Athinarayanan, J.; Periasamy, V. S.; Krishnamoorthy, R.; Alshatwi, A. A. Evaluation of antibacterial and cytotoxic properties of green synthesized Cu_2O/Graphene nanosheets. *Mater. Sci. Eng. C* **2018**, *93*, 242−253.

(32) Athinarayanan, J.; Periasamy, V. S.; Qasem, A. A.; Alshatwi, A. A. Borassus flabellifer biomass lignin: Isolation and characterization of its antioxidant and cytotoxic properties. *Sustainable Chem. Pharm.* **2018**, *10*, 89−96.

(33) Periasamy, V. S.; Athinarayanan, J.; Alfawaz, M. A.; Alshatwi, A. A. Carbon nanoparticle induced cytotoxicity in human mesenchymal stem cells through upregulation of TNF3, NFKBIA and BCL2L1 genes. *Chemosphere* **2016**, *144*, 275−284.

(34) Athinarayanan, J.; Periasamy, V. S.; Alsaif, M. A.; Al-Warthan, A. A.; Alshatwi, A. A. Presence of nanosilica (E551) in commercial food products: TNF-mediated oxidative stress and altered cell cycle progression in human lung fibroblast cells. *Cell Biol. Toxicol.* **2014**, *30*, 89−100.

(35) Yearla, S. R.; Padmasree, K. Preparation and characterisation of lignin nanoparticles: evaluation of their potential as antioxidants and UV protectants. *J. Exp. Nanosci.* **2016**, *11*, 289−302.

(36) Lin, S. Y. Ultraviolet spectrophotometry. In *Methods in lignin chemistry*; Lin, S. Y., Dence, C. W., Eds.; Springer-Verlag: Heidelberg, 1992; pp 215−232.

(37) Chen, Y.; Jiang, Y.; Tian, D.; Hu, J.; He, J.; Yang, G.; Luo, L.; Xiao, Y.; Deng, S.; Deng, O.; Zhou, W.; Shen, F. Fabrication of spherical lignin nanoparticles using acid-catalyzed condensed lignins. *Int. J. Biol. Macromol.* **2020**, *164*, 3038−3047.

(38) Gao, S.; Zhao, J.; Wang, X.; Guo, Y.; Han, Y.; Zhou, J. Lignin structure and solvent effects on the selective removal of condensed units and enrichment of S-type lignin. *Polymers* **2018**, *10*, 967.

(39) Gomide, R. A. C.; de Oliveira, A. C. S.; Rodrigues, D. A. C.; de Oliveira, C. R.; de Assis, O. B. G.; Dias, M. V.; Borges, S. V. Development and characterization of lignin microparticles for physical and antioxidant enhancement of biodegradable polymers. *J. Polym. Environ.* **2020**, *28*, 1326−1334.

(40) Luo, T.; Wang, C.; Ji, X.; Yang, G.; Chen, J.; Yoo, C. G.; Janaswamy, S.; Lyu, G. Innovative production of lignin nanoparticles using deep eutectic solvents for multifunctional nanocomposites. *Int. J. Biol. Macromol.* **2021**, *183*, 781−789.

(41) Raval, N.; Maheshwari, R.; Kalyane, D.; Youngren-Ortiz, S. R.; Chougule, M. B.; Tekade, R. K. Importance of physicochemical characterization of nanoparticles in pharmaceutical product development. In *Basic Fundamentals of Drug Delivery*; Tekade, R. K., Ed.; Academic Press: New York, 2019; pp 369−400.

(42) Ma, M.; Dai, L.; Si, C.; Hui, L.; Liu, Z.; Ni, Y. A facile preparation of super long-term stable lignin nanoparticles from black liquor. *ChemSusChem* **2019**, *12*, 5239−5245.

(43) Green, D.R.; Galluzzi, L.; Kroemer, G. Cell biology. Metabolic control of cell death. *Science* **2014**, *345*, 1250256.

(44) Ullah Khan, A.; Wilson, T. Reactive oxygen species as cellular messengers. *Chem. Biol.* **1995**, *2*, 437−445.

(45) He, L.; He, T.; Farrar, S.; Ji, L.; Liu, T.; Ma, X. Antioxidants maintain cellular redox homeostasis by elimination of reactive oxygen species. *Cell. Physiol. Biochem.* **2017**, *44*, 532−553.

(46) Zheng, L.; Lu, G.; Pei, W.; Yan, W.; Li, Y.; Zhang, L.; Huang, C.; Jiang, Q. Understanding the relationship between the structural properties of lignin and their biological activities. *Int. J. Biol. Macromol.* **2021**, *190*, 291−300.

(47) Liang, R.; Zhao, J.; Li, B.; Cai, P.; Loh, X. J.; Xu, C.; Chen, P.; Kai, D.; Zheng, L. Implantable and degradable antioxidant poly (ε-caprolactone)-lignin nanofiber membrane for effective osteoarthritis treatment. *Biomaterials* **2020**, *230*, 119601.